

# Continuous conversion of CO<sub>2</sub> to alcohols in a TiO<sub>2</sub> photoanode-driven photoelectrochemical system

Sergio Castro, Jonathan Albo\* and Angel Irabien

Department of Chemical & Biomolecular Engineering, University of Cantabria, Avda. Los Castros s/n,  
39005 Santander, Spain

\*Corresponding author, email: [alboj@unican.es](mailto:alboj@unican.es)

## ABSTRACT

### BACKGROUND

The recycling of CO<sub>2</sub> by photo-electrochemical reduction has attracted wide interest due to its potential benefits when compared to electro-, and photo-catalysis approaches. Among the different available semiconductors, TiO<sub>2</sub> is the most employed material in photo-electrochemical cells. Besides, Cu is a well-known electrocatalyst for alcohols production from CO<sub>2</sub> reduction.

### RESULTS

In this study, a photo-electrochemical cell consisting on a TiO<sub>2</sub> photoanode Membrane Electrode Assembly (MEA) and a Cu plate are employed to reduce CO<sub>2</sub> to methanol and ethanol continuously under UV illumination (100 mW·cm<sup>-2</sup>). A maximum increment of 4.3 mA·cm<sup>-2</sup> in current between the illuminated and dark conditions is achieved at -2 V vs. Ag/AgCl. The continuous photo-electrochemical reduction process in the filter-press cell is evaluated in terms of reaction rate ( $r$ ), as well as Faradaic ( $FE$ ) and energy ( $EE$ )

This article has been accepted for publication and undergone full peer review but has not been through the copyediting, typesetting, pagination and proofreading process which may lead to differences between this version and the Version of Record. Please cite this article as doi: [10.1002/jctb.6315](https://doi.org/10.1002/jctb.6315)

efficiencies. At -1.8 V vs. Ag/AgCl, a maximum reaction rate of  $r = 9.5 \mu\text{mol}\cdot\text{m}^{-2}\cdot\text{s}^{-1}$ ,  $FE = 16.2\%$  and  $EE = 5.2\%$  for methanol, and  $r = 6.8 \mu\text{mol}\cdot\text{m}^{-2}\cdot\text{s}^{-1}$ ,  $FE = 23.2\%$  and  $EE = 6.8\%$  for ethanol can be achieved.

## CONCLUSIONS

The potential benefits of the photoanode-driven system, in terms of yields and efficiencies, are observed when employing a  $\text{TiO}_2$ -based MEA photoanode and Cu as dark cathode. The results demonstrate first the effect of UV illumination on current density, and then the formation of alcohols from the continuous photoreduction of  $\text{CO}_2$ . Increasing the external applied voltage led to an enhanced production of methanol, but decreases ethanol formation. The system outperforms previous photoanode-based systems for the  $\text{CO}_2$ -to-alcohols reactions.

**KEYWORDS:** Photoelectrocatalysis;  $\text{CO}_2$  reduction;  $\text{TiO}_2$ ; Cu; methanol, ethanol.

## 1. INTRODUCTION

The concentration of  $\text{CO}_2$  in the atmosphere has increased to worrying levels in recent years, mainly due to fossil fuels burning. This has accelerated research activities to obtain value added products from residual  $\text{CO}_2$ , instead of discard it as a residue.<sup>1</sup> There are different possibilities to convert  $\text{CO}_2$  into valuable products. Among the different technologies available, the electrochemical reduction of  $\text{CO}_2$  has attracted great interest due to the potential economic and environmental benefits. This technology, apart from allowing  $\text{CO}_2$  dissociation at ambient conditions using electricity, is also an excellent alternative to store the intermittent energy produced from renewables in the chemical

bonds.<sup>2</sup> Moreover, the integration of a light source in electrochemical reduction devices (a photoelectrochemical approach, PEC) has attracted an increasing interest recently because it may allow avoiding the interconnections between devices, reducing, in principal, system capital costs and electricity losses.<sup>3</sup> Compared to photocatalysis, the applied bias can cause band bending and help the oriented transfer of the photogenerated electrons, decreasing the recombination of the photogenerated electron-hole pairs. Besides, photocatalytic materials with unfavorable band positions for CO<sub>2</sub> reduction and H<sub>2</sub>O oxidation can be still used in photoelectrocatalytic systems when applying an external bias.

There are different electrode configurations for the PEC systems on dependence on which electrode (i.e., anode, cathode or both) acts as photoelectrode.<sup>4</sup> Photocathode-dark anode has been the most employed configuration.<sup>5-9</sup> In this case, a *p*-type semiconductor is employed as photocathode and a metal as anode. Unfortunately, with the *p*-type semiconductors two-electron products are usually obtained and the system efficiency is low. On the other hand, CO<sub>2</sub> reduction in a photoanode-dark cathode PEC is a simpler configuration and depends on the photoanode and the cathode activity independently<sup>10-12</sup>, and offers the advantage of reducing the external energy requirements of the process.<sup>13</sup> In this configuration, H<sub>2</sub>O oxidation in the photoanode provides electrons and protons for CO<sub>2</sub> reduction in the cathode compartment. Besides, the negative potential voltage generated in the photoanode by the light, supplies an additional negative potential for CO<sub>2</sub> reduction in the cathode.<sup>4</sup> Another PEC photoelectrodes configuration is the combination of a photocathode for CO<sub>2</sub> reduction with a photoanode to deals with H<sub>2</sub>O oxidation (as

represented in Figure 1).<sup>13-15</sup> In contrast to the previous configurations, the main advantage is that with some pairs of materials an external electrical energy supply for the redox reactions may, ideally, not be needed. However, in most cases, the voltage generated by the light source is not enough and a continuous external power supply is required.<sup>16, 17</sup>

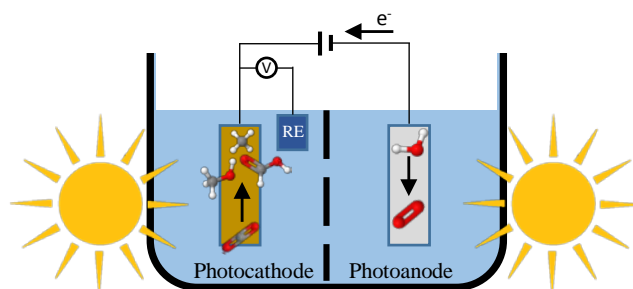


Figure 1. PEC cell in a photocathode-photoanode configuration. Edited from [2].

Moreover, the formation of alcohols from  $\text{CO}_2$  has received increasing attention due to their proper integration in the actual fuel infrastructure, besides being considered an advantageous energy storage and a precursor to synthesize other products.<sup>18-20</sup> Methanol ( $\text{CH}_3\text{OH}$ ) is considered an excellent energy intermediate due to the stable storage properties and its high energy density. In addition to the application as a fuel,  $\text{CH}_3\text{OH}$  is an intermediate to other bulk chemicals employed in everyday life products like plastics and paints.<sup>21</sup> Ethanol ( $\text{C}_2\text{H}_5\text{OH}$ ) is an important raw material with high heating value usually employed in disinfectants and organics material.<sup>22</sup> It can also replace fossil fuels in a key sector such as the transport industry.<sup>23</sup> Thus, both products offer an alternative to deal with climate change,

reducing our dependence on fossil fuels and allowing CO<sub>2</sub> recycling in a neutral carbon cycle.

18,24

TiO<sub>2</sub> is the most employed semiconductor in photo-assisted processes.<sup>25-28</sup> It is a *n*-type semiconductor that possesses a wide band gap (3.0 eV) and mainly absorb UV light.<sup>29</sup>

This semiconductor has been considered a cheaper and more environmental friendly material<sup>30</sup> since the first report in 1979.<sup>25</sup> Besides, Cu has demonstrated to possess the capacity to produce hydrocarbons and alcohols from CO<sub>2</sub>.<sup>31</sup> In particular, previous works from our group employed a Cu plate for CO<sub>2</sub> electroreduction, with a reaction rate of CH<sub>3</sub>OH of  $r = 8.7 \mu\text{mol}\cdot\text{m}^{-2}\cdot\text{s}^{-1}$  and a  $FE = 4.6 \%$  at -1.3V vs. Ag/AgCl. These values were subsequently enhanced by using Cu oxide<sup>31, 32</sup> and metal-organic frameworks (MOFs)-based electrodes at different experimental conditions in continuous operation mode.<sup>18, 31-33</sup>

Thus, the aim of the present work is coupling a TiO<sub>2</sub>-based photoanode in an electrochemical filter press cell for the continuous conversion of CO<sub>2</sub> to alcohols (i.e. CH<sub>3</sub>OH and C<sub>2</sub>H<sub>5</sub>OH) in order to reduce the requirements of external energy, and so reduce energy consumption. A Cu plate is used as dark cathode for designing a reliable photoanode-dark cathode configuration for CO<sub>2</sub> photoreduction. The specific objectives are as follows: (1) to prepare and optimize a TiO<sub>2</sub>-based photoanode, (2) to adapt an electrochemical cell for the PEC conversion of CO<sub>2</sub> to alcohols, and finally (3) to analyze the effect of voltage on process performance. The results are considered a step further in the development of continuous CO<sub>2</sub> conversion processes under the sun.

## 2. EXPERIMENTAL SECTION

## 2.1. TiO<sub>2</sub> photoanode preparation

A TiO<sub>2</sub> photoanode is fabricated by air-brushing an ink composed by a mixture of TiO<sub>2</sub> (Sigma Aldrich, P25), Nafion (Alfa Aesar 5wt%) as binder and isopropanol (99.5%, Sigma Aldrich) as vehicle, with a 70:30 wt% TiO<sub>2</sub>/Nafion ratio in a 3 wt.% of solid in the final isopropanol dispersion onto a Toray carbon paper (TGP-H60). An ultrasound bath is used to homogenize the mixture. The TiO<sub>2</sub> loading varies from 1 to 3 mg·cm<sup>-2</sup>. The TiO<sub>2</sub> photoanode is coupled by hot-pressing with a Nafion membrane (Nafion 117), previously activated in HCl for 30 minutes and rinsed with deionized water before use, forming a Membrane Electrode Assembly (MEA) able to enhance H<sup>+</sup> transport, reducing mass transfer limitations.<sup>33,35</sup>

## 2.2. Photoelectroreduction cell and experimental conditions

The continuous PEC reduction of CO<sub>2</sub> is carried out using a commercial filter press cell reactor (Electrocell, Denmark), employing a Cu plate as cathode and the prepared MEA as photoanode, which also separates the cell compartments. A 1 M KOH aqueous solution is used as catholyte and anolyte and a cold UV LED light (100 mW·cm<sup>-2</sup>) to illuminate the photoactive area (10 cm<sup>2</sup>) of the TiO<sub>2</sub> photoanode. In the cathode side, there are two inputs: the catholyte and the CO<sub>2</sub> gas; and one output: the catholyte with the reaction products (liquid and gaseous). The Cu plate works as working electrode, the TiO<sub>2</sub> photoelectrode as counter electrode and Ag/AgCl as reference electrode. The CO<sub>2</sub> reduction is conducted at ambient conditions. Figure 2 shows a scheme of the experimental setup, while Figure 3 shows a detailed view of the cell configuration. The experimental system

includes four tanks for inlet and outlet electrolyte solutions, two peristaltic pumps to circulate the liquid at a flow rate of  $10 \text{ ml}\cdot\text{min}^{-1}$ , two pressure indicators and mass-flow controllers to fix the  $\text{CO}_2$  inlet flow rate at  $180 \text{ ml}\cdot\text{min}^{-1}$ . Moreover, a potentiostat (AutoLabPGSTAT 302N) is used. The PEC behavior of the  $\text{TiO}_2$  photoanodes is evaluated in a one-compartment glass at a scan rate of  $50 \text{ mV}\cdot\text{s}^{-1}$  after 20 cycles with and without light illumination.

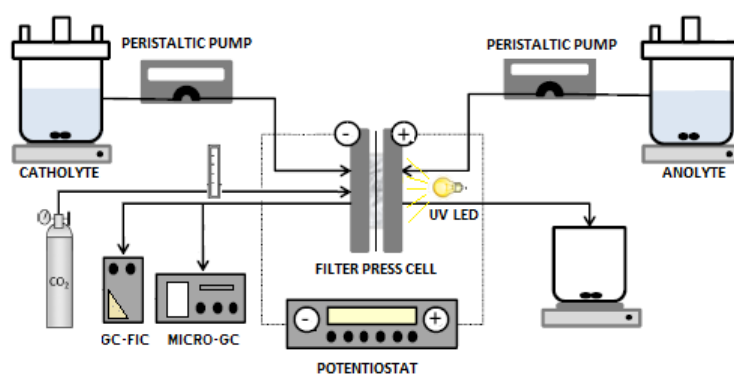


Figure 2. Experimental system for the continuous PEC reduction of  $\text{CO}_2$ . Edited from [36].

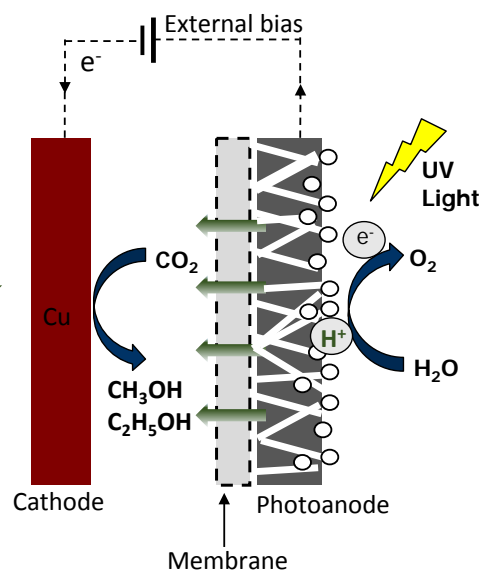


Figure 3. Detail of the PEC cell configuration. Edited from ref. [32].

Continuous experiments in the PEC cell are performed by duplicate during 50 minutes. Both liquid and gas samples are taken every 10 minutes, and a final average concentration is calculated for each test. The values that are two times lower/higher than the average value are discarded in order to calculate the reaction rate ( $r$ ) and the Faraday efficiency ( $FE$ ) with an error less than 10%. The values are normalized to reacting  $\text{CO}_2$  (inlet-outlet) in the system and adjusted to a  $FE= 100\%$ . To collect the gaseous samples, the experimental system is pressurized to 0.2 bar for its subsequent analysis in an in-line gas microchromatograph (3000 Micro GC, Inficon). Liquid samples are analysed in a gas chromatograph (GCMSQP2010 Ultra Shimadzu) equipped with a flame ionization detector (FID). The reaction rate shows the formation rate for every product per unit of



area and time ( $\mu\text{mol}\cdot\text{m}^{-2}\cdot\text{s}^{-1}$ ) and the  $FE$  is defined as the selectivity of the reaction to form each products, calculated according to the Ec 1:

$$FE (\%) = \frac{z \cdot n \cdot F}{q} \times 100 \quad [Ec \ 1]$$

where  $z$  is the theoretical number of  $e^-$  exchanged to form the desired product,  $n$  is the number of moles produced,  $F$  is the Faraday constant ( $F = 96,485 \text{ C}\cdot\text{mol}^{-1}$ ) and  $q$  is the total charge applied in the process. Moreover, the energy efficiency,  $EE$ , which indicates the total energy used toward the formation of the desired products can be calculated according to the following equation (Ec 2):

$$EE (\%) = \frac{E_T}{E} \times FE \quad [Ec \ 2]$$

Where  $E$  is the real potential applied in the system and  $E_T$  the theoretical potential needed for the formation of  $\text{CH}_3\text{OH}$  ( $-0.58 \text{ V vs. Ag/AgCl}$ ) and  $\text{C}_2\text{H}_5\text{OH}$  ( $-0.53 \text{ V vs. Ag/AgCl}$ ).

### 3. RESULTS AND DISCUSSION

#### 3.1. Photoelectrochemical behavior of the $\text{TiO}_2$ photoelectrode

Figure 4a shows the photocurrent response of the  $\text{TiO}_2$  photoanode MEA during on-off illumination cycles in a one-compartment glass under  $100 \text{ mW}\cdot\text{cm}^{-2}$  of UV illumination at  $-1.8 \text{ V vs. Ag/AgCl}$  in the presence of  $\text{CO}_2$ , while Figure 4b shows the current densities observed with and without illumination in cell when  $\text{CO}_2$  is continuously bubbling in a potential range between  $-1.2 \text{ V}$  and  $-2 \text{ V vs. Ag/AgCl}$  and a  $\text{TiO}_2$  loading of  $3 \text{ mg}\cdot\text{cm}^{-2}$ , where an optimal reduction of  $\text{CO}_2$  to alcohols can be expected.<sup>34, 37, 38</sup> It should be noted

that the TiO<sub>2</sub>-based photoanodes showed no changes in response (current) during on-off cycles when illuminated with a visible LED light (100 mW·cm<sup>-2</sup>).

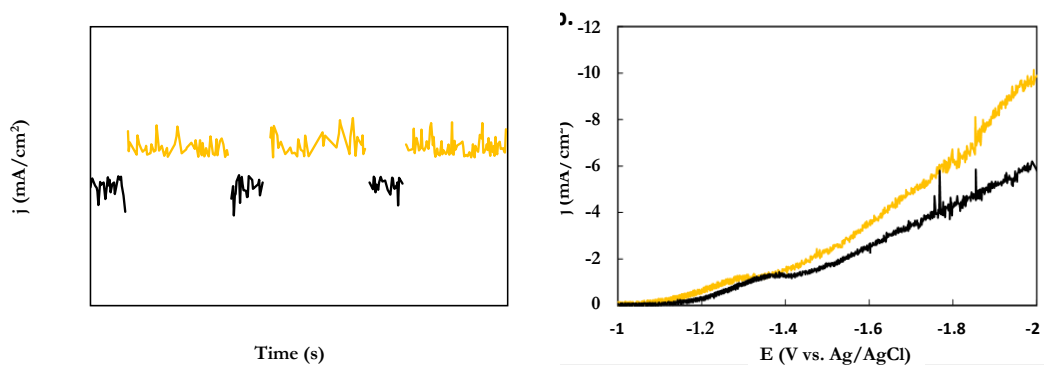


Figure 4. (a) On-off cycles for the TiO<sub>2</sub> photoanode MEA in the dark (black) and under UV illumination (yellow) with CO<sub>2</sub> at -1.8 V vs. Ag/AgCl and, (b)  $j$ - $E$  characteristics of the TiO<sub>2</sub> MEA photoanode in the dark (black) and under UV illumination (yellow) with CO<sub>2</sub>.

First, the current density of the system under UV light results larger than in the dark conditions in on-off cycles (Figure 4a) at -1.8 V vs. Ag/AgCl. Then, figure 4b shows that the increase in current density under UV light illumination can be observed in all the potential range evaluated. The variation in current density between the illuminated and dark conditions represents the highest attainable photocurrent in the system. Of course, increases in current density are associated to higher voltage values, getting a maximum increment of  $j= 4.3 \text{ mA}\cdot\text{cm}^{-2}$  under UV illumination ( $j= 9.9 \text{ mA}\cdot\text{cm}^{-2}$ ) respect to the dark experiment at -2 V vs. Ag/AgCl ( $j= 5.6 \text{ mA}\cdot\text{cm}^{-2}$ ), although this high potential could not

be beneficial for alcohols production.<sup>36</sup> These results may be taken as a first indication for an enhanced PEC process performance as evaluated hereafter.

### 3.2. Process performance of the TiO<sub>2</sub>/Nafion/Cu plate system

The products obtained for the continuous CO<sub>2</sub> reduction PEC reduction employing a TiO<sub>2</sub>-based MEA as photoanode and a Cu plate as cathode are alcohols (i.e. CH<sub>3</sub>OH and C<sub>2</sub>H<sub>5</sub>OH) together with CO and C<sub>2</sub>H<sub>4</sub>. Their formation, and so process performance, is evaluated in terms of  $r$  and  $FE$ . Figure 5 initially shows an example of the evolution of  $j$  during the experimental time (UV illumination).

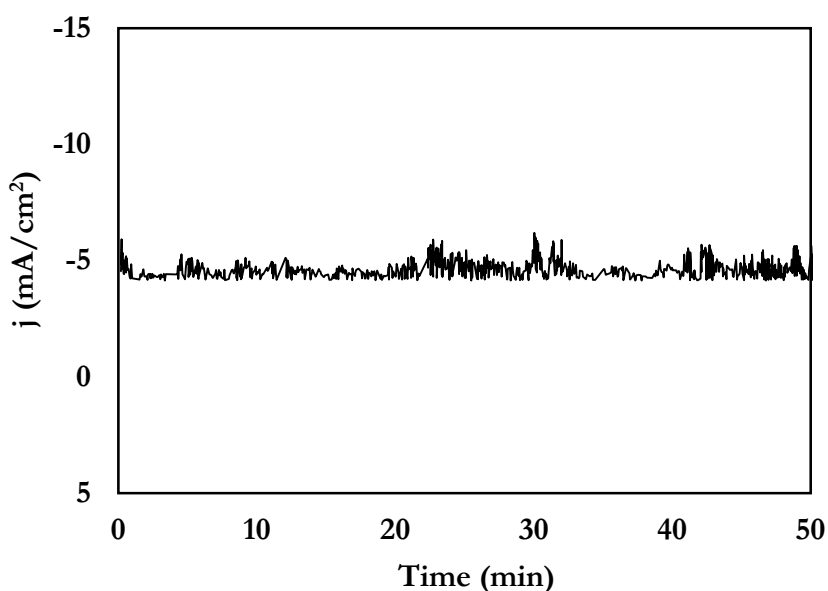


Figure 5. PEC activity,  $j$ , with time at -1.8 V vs. Ag/AgCl.

As can be observed, the system presents a pseudo-stable activity after 50 min of operation in the continuous liquid-liquid CO<sub>2</sub> PEC conversion. The small fluctuations observed are

commonly caused by the direct input of CO<sub>2</sub> gas into the cathode compartment, as well as the production of gaseous products (bubbles) on the electrode surface. The results also give an idea of the stability of the system, although, of course, longer-term tests would be needed in order to assess the feasibility of the system for real applications.

Among the different key variables of the process, the TiO<sub>2</sub> catalyst loading can have a remarkable impact on process performance.<sup>35</sup> In principle, the higher the semiconductor surface, the greater the photocurrent generated as more electrons are excited in the photoanode.

Therefore, figure 6 shows the *FE* values at three different TiO<sub>2</sub> catalyst loadings in the MEA (i.e. 1, 2 and 3 mg·cm<sup>-2</sup>).

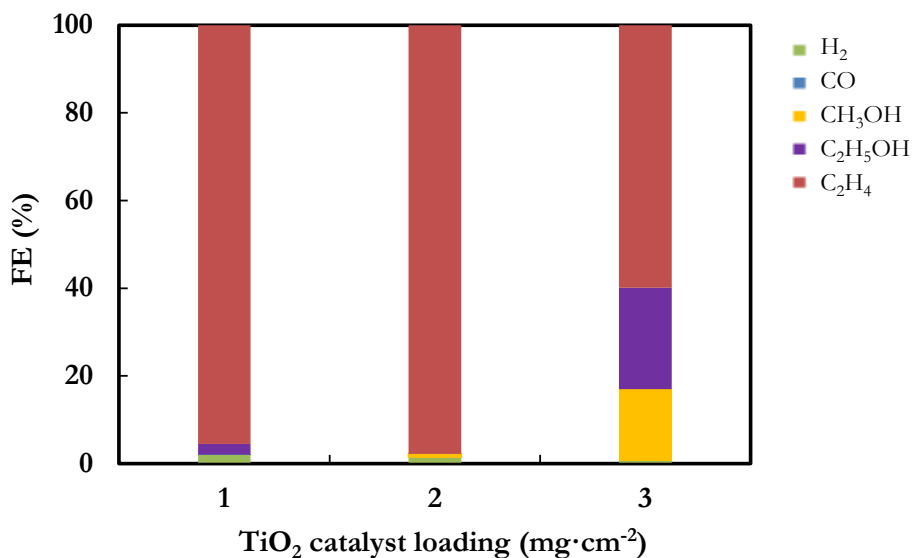


Figure 6. Effect of TiO<sub>2</sub> loading in the photoanode.

As observed,  $3 \text{ mg}\cdot\text{cm}^{-2}$  seems to be the optimum for both,  $\text{CH}_3\text{OH}$  and  $\text{C}_2\text{H}_5\text{OH}$  formation, with a *FE* value of 16.2 % and 23.2%, respectively, in comparison to the value observed at  $1 \text{ mg}\cdot\text{cm}^{-2}$ , where no  $\text{CH}_3\text{OH}$  was detected and a  $\text{C}_2\text{H}_5\text{OH}$  *FE* value of 2.4 % can be achieved. At higher catalyst loadings than  $3 \text{ mg}\cdot\text{cm}^{-2}$ , Seger et al.<sup>34</sup> found that the light absorption limits the photocurrent generation due to particle agglomeration which hampers the accessibility of the light to the catalytic surface. Consequently, a  $\text{TiO}_2$  loading of  $3 \text{ mg}\cdot\text{cm}^{-2}$  is recommended to get the best performance in the developed  $\text{TiO}_2$  photoanode MEA-driven system for  $\text{CO}_2$  PEC conversion and is applied hereafter.

Then, the values for alcohols (i.e.  $\text{CH}_3\text{OH}$  and  $\text{C}_2\text{H}_5\text{OH}$ ) formation in a voltage range from -1.2 to -2 V vs. Ag/AgCl are presented in Table 1, while Figure 7 shows the *FE* to all liquid and gas-phase products detected as a function of the applied voltage.

The values in Table 1 are normalized by the total charge  $q$  (C) passing through the system in order to properly analyze the PEC activity. The values are also compared with our previous findings for the electrochemical conversion of  $\text{CO}_2$  (in the dark) using a Cu plate.<sup>31</sup>

Table 1. Production rates,  $r$ , for alcohols at different  $E$  employing a Cu plate as cathode.

E (V)	j ( $\text{mA}\cdot\text{cm}^{-2}$ )	q (C)	r ( $\mu\text{mol}\cdot\text{m}^{-2}\cdot\text{s}^{-1}$ )		r · C <sup>-1</sup> x10 <sup>-8</sup>	
			CH <sub>3</sub> OH	C <sub>2</sub> H <sub>5</sub> OH	CH <sub>3</sub> OH	C <sub>2</sub> H <sub>5</sub> OH
-1.2	0.1	6	-	19.3	-	321.6
-1.4	1.6	21.6	-	13.9	-	64.3
-1.6	1	20.7	-	14.9	-	71.9
-1.8	5.9	102	9.5	6.8	9.3	6.6
-2	9.8	117.6	24	-	20.4	-
-1.3*	10.8	584.8	8.7	-	1.5	-

-1.5\*      16.6      894.2      23      -      2.6      -

\*Cu plate cathode-Pt anode. Q/A= 2 ml·min<sup>-1</sup>·cm<sup>-2</sup> in an electrochemical system. <sup>31</sup>

First, the data shows that the current densities values in the PEC system are significantly reduced (for a comparable production of alcohols) to those at a Cu plate and a Pt anode in an electrochemical system (in the dark), which might initially indicate an enhancement in energy efficiency. Then, the reaction rate values,  $r$ , show similar ranges for CH<sub>3</sub>OH for the same voltage level in electrochemical and PEC experiments. The  $r \cdot C^{-1}$  values obtained in this work, however, are clearly superior in PEC ( $r = 9.3 \mu\text{mol} \cdot \text{m}^{-2} \cdot \text{s}^{-1} \cdot \text{C}^{-1}$  for CH<sub>3</sub>OH at -1.8 V vs. Ag/AgCl) in comparison to those achieved in the electrochemical experiments ( $r = 2.6 \mu\text{mol} \cdot \text{m}^{-2} \cdot \text{s}^{-1} \cdot \text{C}^{-1}$  for CH<sub>3</sub>OH) at similar voltage level, showing the benefits of the PEC. The PEC system seems also to be beneficial for the formation of C<sub>2</sub>H<sub>5</sub>OH, which requires a higher number of electrons and C-C coupling. This enhancement of CO<sub>2</sub> reduction to alcohols can be generally associated with two phenomena: first, the cathode potential becoming more negative (higher supply of e<sup>-</sup>) and then, the large amount of H<sup>+</sup> generation from water the photo-electrolysis, that seem to be available for CO<sub>2</sub> conversion to alcohols in the cathode. <sup>11</sup> The *FE* to both alcohols notably decrease at -2 V vs. Ag/AgCl, which can be ascribed to an enhanced formation of C<sub>2</sub>H<sub>4</sub> (Figure 7).

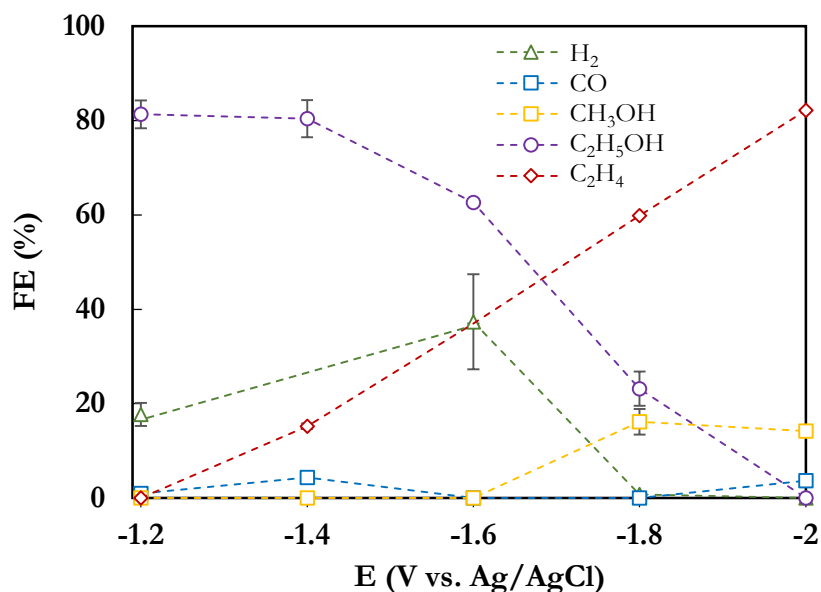


Figure 7. *FE* for all liquid and gas-phase products obtained at different *E*.

The highest *FE* to CH<sub>3</sub>OH is achieved at -1.8 V vs. Ag/AgCl, *FE*= 16.2 %. In the other hand, the *FE* to C<sub>2</sub>H<sub>5</sub>OH is negatively affected by increases in *E*, going from *FE*= 81% at -1.2 V to 23.2 % at -1.8 V vs. Ag/AgCl, in agreement with the values shown in Table 1. These *FE* values towards C<sub>2</sub>H<sub>5</sub>OH, exceed those previously reported for other promising Cu-based systems, such as Cu-based MOF materials supported on GDEs (*FE*~ 6% at -10 mA·cm<sup>-2</sup> in [Cu<sub>3</sub>(μ<sub>6</sub>-C<sub>9</sub>H<sub>3</sub>O<sub>6</sub>)<sub>2</sub>]<sub>n</sub>).<sup>36</sup>

Besides, the formation of C<sub>2</sub>H<sub>4</sub> can be expected in the potential range tested, as previously found in our group for the gas-phase CO<sub>2</sub> reduction at Cu-based surfaces, achieving a *FE*= 91% to C<sub>2</sub>H<sub>4</sub> at -2.1 V vs. Ag/AgCl<sup>33</sup> as also reported by other authors.<sup>39,40</sup> Overall, an applied voltage of -1.8 V vs. Ag/AgCl is preferred for the formation of both alcohols.

Furthermore, Table 2 summarizes *EEs* achieved for alcohols as a function of the applied potential.

Table 2. Energy efficiency (*EE*) for CH<sub>3</sub>OH and C<sub>2</sub>H<sub>5</sub>OH.

E(V) vs. Ag/AgCl	<b>EE (%)</b>						
	-1.2	-1.4	-1.6	-1.8	-2	-1.3*	-1.5*
CH <sub>3</sub> OH	-	-	-	5.2	4.1	2	1.4
C <sub>2</sub> H <sub>5</sub> OH	35.9	30.4	20.7	6.8	-	-	-

\*Cu plate cathode-Pt anode. Q/A=2 ml·min<sup>-1</sup>·cm<sup>-2</sup> employing an electrochemical system. <sup>31</sup>

As observed, a maximum *EE* for CH<sub>3</sub>OH can be obtained at -1.8 V vs. Ag/AgCl (*EE*=5.2%), while lowering the voltage applied seems beneficial for C<sub>2</sub>H<sub>5</sub>OH production (*EE*=35.9% at -1.2 V vs. Ag/AgCl). These results are clearly superior to the maximum *EE* values obtained in Cu plate-based system for the electrochemical reduction of CO<sub>2</sub> (in the dark).

Finally, the best performance results obtained at -1.8 V vs. Ag/AgCl are compared (in terms of *r* and *FE*) with previous reports for alcohols production in photoanode-dark cathode PEC systems in Table 3. As observed, the formation of CH<sub>3</sub>OH and C<sub>2</sub>H<sub>5</sub>OH achieved using a TiO<sub>2</sub> photoanode MEA- Cu cathode configuration from this work are, in general, higher than those previously reported for CH<sub>3</sub>OH production, and are only exceeded by the value recorded by Hasan et al.<sup>41</sup> with a cathode of Pt and a photoanode of Cu-RGO-TiO<sub>2</sub>/ITO. It should be also taken into account that others variables (i.e. reaction medium, cell configuration, experimental conditions, etc.) may affect the results. Besides, the *FE* to C<sub>2</sub>H<sub>5</sub>OH achieved in this work clearly surpass others in literature (except the results from Hasan et al.<sup>41</sup>) employing the PEC configuration.



Table 3. Production of alcohols from CO<sub>2</sub> in a photoanode-dark cathode configuration.

Cathode	Photoanode	Light source/ Intensity	E (V vs. Ag/AgCl)	j (mA·cm <sup>-2</sup> )	r (μmol·m <sup>-2</sup> ·s <sup>-1</sup> )	FE (%)	Ref.
Cu plate	TiO <sub>2</sub>	UV LED (λ =365; 100 mW·cm <sup>-2</sup> )	-1.8	5.9	CH <sub>3</sub> OH: 9.5 C <sub>2</sub> H <sub>5</sub> OH: 6.8	CH <sub>3</sub> OH: 16.2 C <sub>2</sub> H <sub>5</sub> OH: 23.2	[This work]
Cu	TiO <sub>2</sub>	AM 1.5G (100 mW·cm <sup>-2</sup> )	-0.7	1.36	-	CH <sub>3</sub> OH: 1.1	[43]
Pt/CF	TiO <sub>2</sub>	300 W Xe arc lamp (320 nm<λ>410 nm)	-1.95	-	CH <sub>3</sub> OH: 0.41 C <sub>2</sub> H <sub>5</sub> OH: 1.25	CH <sub>3</sub> OH: 5 C <sub>2</sub> H <sub>5</sub> OH: 29	[4]
Pt	Cu-RGO- TiO <sub>2</sub> /ITO	150 W Xe arc lamp	-0.56	1.31	CH <sub>3</sub> OH: 525.16	CH <sub>3</sub> OH: 32.5	[41]
Pt-RGO	Pt-TNT*	300 W Xe-arc lamp	-1.95	-	CH <sub>3</sub> OH: 0.14	CH <sub>3</sub> OH: 5	[10]
Pt-RGO	Pt (5%)-TNT	300 W Xe arc lamp (320 nm<λ>410 nm)	-1.95	-	CH <sub>3</sub> OH: 0.21 C <sub>2</sub> H <sub>5</sub> OH: 0.78	-	[12]
Pt-RGO	Pt-TNT	300 W Xe arc lamp (320 <λ>410 nm)	-1.95	-	CH <sub>3</sub> OH: 2.43 C <sub>2</sub> H <sub>5</sub> OH: 3.75	-	[42]

\*TNT: TiO<sub>2</sub> nanotubes.

#### 4. CONCLUSIONS

Coupling light to electrochemical devices for CO<sub>2</sub> conversion is an interesting approach to obtain value added products under the sun, solving the issues related to global warming at the same time. When the continuous photoelectrochemical transformation of CO<sub>2</sub> is carried out in a filter-press cell employing a TiO<sub>2</sub> MEA photoanode, a maximum increase

of  $4.3 \text{ mA}\cdot\text{cm}^{-2}$  in current density is observed under UV illumination, denoting the potential benefits of the developed photoanode-driven system for an enhanced energy efficiency. Methanol and ethanol, as well as hydrogen, carbon monoxide and ethylene, are detected as liquid and gas-phase products in the system employing a Cu plate as cathode. At  $-1.8 \text{ V}$  vs. Ag/AgCl, the maximum production of methanol is  $9.5 \text{ }\mu\text{mol}\cdot\text{m}^{-2}\cdot\text{s}^{-1}$ , the Faradaic efficiency is 16.2 % and the energy efficiency 5.2 %. In case of ethanol, a reaction rate of  $6.8 \text{ }\mu\text{mol}\cdot\text{m}^{-2}\cdot\text{s}^{-1}$ , a Faradaic efficiency of 12.1 % and energy efficiency of 6.8 % can be achieved for a  $\text{TiO}_2$  loading of  $3 \text{ mg}\cdot\text{cm}^{-2}$  in the photoanode. In general, methanol production results are enhanced at higher voltages, while ethanol production seems to be negatively affected. All in all, the developed  $\text{TiO}_2$  photoanode-driven system is able to enhance the production of alcohols from  $\text{CO}_2$  under UV light, reducing the energy required in the process compared to an electrochemical system.

## 5. ACKNOWLEDGEMENTS

The authors gratefully acknowledge the financial support from the Spanish Ministry of Economy and Competitiveness (MINECO) through the projects CTQ2016- 76231-C2-1-R and Ramón y Cajal programme (RYC-2015-17080).

## 6. REFERENCES

1. Goeppert A, Czaun M, Jones JP, Prakash GKS and Olah GA. Recycling of carbon dioxide to methanol and derived products-closing the loop. *Chem Soc Rev* **43**: 7995-8048 (2014).
2. Castro S, Albo J and Irabien A. Photoelectrochemical reactors for CO<sub>2</sub> utilization. *ACS Sustainable Chem Eng* **6**, **12**: 15877-15894 (2018).
3. Das S and Daud WMA. Photocatalytic CO<sub>2</sub> transformation into fuel: A review on advances in photocatalyst and photoreactor. *Renew Sust Energy Rev* **39**: 765-805 (2014).
4. Zhang M, Cheng J, Xuan X, Zhou J and Cen K. CO<sub>2</sub> Synergistic Reduction in a Photoanode-Driven Photoelectrochemical Cell with a Pt-Modified TiO<sub>2</sub> Nanotube Photoanode and a Pt Reduced Graphene Oxide Electrocathode. *ACS Sustain. Chem Eng* **4**: 6344-6354 (2016).
5. Halmann M. Photoelectrochemical reduction of aqueous carbon dioxide on *p*-type gallium phosphide in liquid junction solar cells. *Nature* **275**: 115-116 (1978).
6. Xia S, Meng Y, Zhou X, Xue J, Pan G, Ni Z. Ti/ZnO-Fe<sub>2</sub>O<sub>3</sub> composite: Synthesis, characterization and application as a highly efficient photoelectrocatalyst for methanol from CO<sub>2</sub> reduction. *Appl Catal B* **187**: 122-133 (2016).
7. Wood J, Summers H, Clark A, Kaeffer N, Braeutigam M, Carbone L, D'Amario L, Fan K, Farre Y, Narbey S, Oswald F, Stevens A, Parmenter DJ, Fay W, La Torre A. A comprehensive comparison of dye-sensitized NiO photocathodes for solar energy conversion. *Phys Chem Phys* **18**: 10727-10738 (2016).

8. Qin G, Zhang Y, Keb X, Tong X, Sun Z, Liang M, Xue S. Photocatalytic reduction of carbon dioxide to formic acid, formaldehyde, and methanol using dye-sensitized TiO<sub>2</sub> film. *Appl Catal B* **129**: 599-605 (2013).
9. Kaneco S, Katsumata H, Suzuki T, Ohta K. Photoelectrocatalytic reduction of CO<sub>2</sub> in LiOH/methanol at metal-modified p-InP electrodes. *Appl Catal B* **64**: 139-145 (2006).
10. Cheng J, Zhang M, Wu G, Wang X, Zhou J, Cen K. Photoelectrocatalytic Reduction of CO<sub>2</sub> into Chemicals Using Pt-Modified Reduced Graphene Oxide Combined with Pt-Modified TiO<sub>2</sub> Nanotubes. *Environ Sci Technol* **48**: 7076-7084 (2014).
11. Cheng J, Zhang M, Liu J, Zhou J, Cen K. Cu foam cathode used as Pt-RGO catalyst matrix to improve CO<sub>2</sub> reduction in a photoelectrocatalytic cell with TiO<sub>2</sub> photoanode. *J Mater Chem A* **3**: 12947-12957 (2015).
12. Chang X, Wang T, Zhang P, Wei Y, Zhao J and Gong J. Stable Aqueous Photoelectrochemical CO<sub>2</sub> Reduction by a Cu<sub>2</sub>O Dark Cathode with Improved Selectivity for Carbonaceous Products. *Angew Chem Int Ed* **55**: 1-6 (2016).
13. Xie S, Zhang Q, Liu G and Wang Y. Photocatalytic and photoelectrocatalytic reduction of CO<sub>2</sub> using heterogeneous catalysts with controlled nanostructures. *Chem Commun* **52**: 35-59 (2016).
14. Sato S, Arai T, Morikawa T, Uemura K, Suzuki M, Tanaka H, Kajino T. Selective CO<sub>2</sub> Conversion to Formate Conjugated with H<sub>2</sub>O Oxidation Utilizing Semiconductor/Complex Hybrid Photocatalysts. *J Am Chem Soc* **133**: (2011).

15. La Tempa TJ, Rani S, Bao N, Grimes CA. Generation of fuel from CO<sub>2</sub> saturated liquids using a p-Si nanowire // n-TiO<sub>2</sub> nanotube array photoelectrochemical cell. *Nanoscale* **4**: 2245-2250 (2012).
16. Weng B, Wei W, Wu H, Alenizi AM, Zheng G. Bifunctional CoP and CoN Porous Nanocatalysts Derived from ZIF-67 In Situ Grown on Nanowire Photoelectrodes for Efficient Photoelectrochemical Water Splitting and CO<sub>2</sub> Reduction. *J Mater Chem A* **4**: 15353-1536 (2016).
17. Sahara G, Kumagai H, Maeda K, Kaeffer N, Artero V, Higashi M, Abe R, Ishitani O. Photoelectrochemical Reduction of CO<sub>2</sub> Coupled to Water Oxidation Using a Photocathode With a Ru(II)–Re(I) Complex Photocatalyst and a CoO<sub>x</sub>/TaON Photoanode. *J Am Chem Soc* **138**: 14152-14158 (2016).
18. Albo J, Alvarez-Guerra M, Castaño P and Irabien A. Towards the electrochemical conversion of carbon dioxide into methanol. *Green Chem* **17**: 2304-2324 (2015).
19. Albo J, Perfecto-Irigaray M, Beobide G, Irabien A. Cu/Bi metal-organic framework-based systems for an enhanced electrochemical transformation of CO<sub>2</sub> to alcohols. *Journal of CO<sub>2</sub> Utilization* **33**: 157-165 (2019).
20. Olah GA. Beyond Oil and Gas: The Methanol Economy. *Angew Chem Int Ed* **44**: 2636-2639 (2005).
21. Le M, Ren M, Zhang Z, Sprunger PT, Kurtz RL and Flake JC. Electrochemical reduction of CO<sub>2</sub> to CH<sub>3</sub>OH at copper oxide surfaces. *J Electrochem Soc* **158**: E45-E49 (2011).

22. Liu Y, Zhang Y, Cheng K, Quan X, Fan X, Su Y, Chen S, Zhao H, Zhang Y, Yu H and Hoffmann MR. Selective Electrochemical Reduction of Carbon Dioxide to Ethanol on a Boron- and Nitrogen-Co-doped Nanodiamond. *Angew Chem* **129**: 15813-15817 (2017).
23. Nitopi S, Bertheussen E, Scott SB, Liu X, Engstfeld AK, Horch S, Seger B, Stephens IEL, Chan K, Hahn C, Nørskov JK, Jaramillo, TF and Chorkendorff I. Progress and Perspectives of Electrochemical CO<sub>2</sub> Reduction on Copper in Aqueous Electrolyte. *Chem Rev* **119**: 7610-7672 (2019).
24. Yuan J, Yang MP, Zhi WY, Wang H, Wang H, Lu JX. Efficient electrochemical reduction of CO<sub>2</sub> to ethanol on Cu nanoparticles decorated on N-doped graphene oxide catalysts. *J of CO<sub>2</sub> Utilization* **33**: 452-460 (2019).
25. Inoue T, Fujishima A, Konishi S, Honda K. Photoelectrocatalytic reduction of carbon dioxide in aqueous suspensions of semiconductor powders. *Nature* **277**: 637-638 (1979).
26. Liu L, Zhao H, Andino JM, Li Y. Photocatalytic CO<sub>2</sub> Reduction with H<sub>2</sub>O on TiO<sub>2</sub> Nanocrystals: Comparison of Anatase, Rutile, and Brookite Polymorphs and Exploration of Surface Chemistry. *ACS Catal* **2(8)**: 1817-1828 (2012).
27. Wang T, Meng X, Li P, Ouyang S, Chang K, Liu G, Meia Z, and Ye J. Photoreduction of CO<sub>2</sub> over the well-crystallized ordered mesoporous TiO<sub>2</sub> with the confined space effect. *Nano Energy* **9**: 50-60 (2014).
28. Zhao H, Pan F, and Li Y. A review on the effects of TiO<sub>2</sub> surface point defects on CO<sub>2</sub> photoreduction with H<sub>2</sub>O. *J Materiomics* **3**: 17-32 (2017).

29. Ibrahim N, Kamarudin SK, Minggu LJ. Biofuel from biomass via photo-electrochemical reactions: An overview. *J Power Sources* **259**, 33-42 (2014).
30. Habisreutinger SN, Schmidt-Mende L, Stolarczyk JK. Photocatalytic reduction of CO<sub>2</sub> on TiO<sub>2</sub> and other semiconductors. *Angew Chem Int Ed* **52**: 2-39 (2013).
31. Albo J, Sáez A, Solla-Gullón J, Montiel V, Irabien A. Production of methanol from CO<sub>2</sub> electroreduction at Cu<sub>2</sub>O and Cu<sub>2</sub>O/ZnO-based electrodes in aqueous solution. *Applied Catalysis B: Environmental* **176-177**: 709-717 (2015).
32. Albo J, Irabien A. Cu<sub>2</sub>O-loaded gas diffusion electrodes for the continuous electrochemical reduction of CO<sub>2</sub> to methanol. *Journal of Catalysis* **343**: 232-239 (2016).
33. Merino-Garcia I, Albo J and Irabien A. Tailoring gas-phase CO<sub>2</sub> electroreduction selectivity to hydrocarbons at Cu nanoparticles. *Nanotechnology* **29**: 014001 (2018).
34. Seger B and Kamat PV. Fuel Cell Geared in Reverse: Photocatalytic Hydrogen Production Using a TiO<sub>2</sub>/Nafion/Pt Membrane Assembly with No Applied Bias. *J Phys Chem C* **113**: 18946-18952 (2009).
35. Merino-Garcia I, Albo J and Irabien A. Productivity and Selectivity of Gas-Phase CO<sub>2</sub> Electroreduction to Methane at Copper Nanoparticle-Based Electrodes. *Energy Technol* **5**: 922 (2017).
36. Albo J, Vallejo D, Beobide G, Castillo O, Castaño P and Irabien A. Copper-Based Metal–Organic Porous Materials for CO<sub>2</sub> Electrocatalytic Reduction to Alcohols. *Chem Sus Chem* **9**: 1-11 (2016).
37. Qiao J, Liu Y, Hong F and Zhang J. A review of catalysts for the electroreduction of carbon dioxide to produce low-carbon fuels. *Chem Soc Rev* **43**: 631-675 (2014).

38. Irabien A, Alvarez-Guerra M, Albo J and Dominguez-Ramos A, Electrochemical Conversion of CO<sub>2</sub> to Value-Added Products, in *Electrochemical water and wastewater treatment*, ed by Martínez-Huitle CA, Rodrigo MA and Scialdone O. Elsevier Inc. pp 29-59 (2018).
39. Komatsu S, Tanaka M, Okumura A, Kungi A. Preparation of cu-solid polymer electrolyte composite electrodes and application to gas-phase electrochemical reduction of CO<sub>2</sub>. *Electrochim Acta* **40**: 745-753 (1995).
40. Cook RL, Macduff RC, Sammells AF. High Rate Gas Phase CO<sub>2</sub> Reduction to Ethylene and Methane Using Gas Diffusion Electrodes. *J Electrochem Soc* **137**: 607-608 (1990).
41. Hasan M.R, Hamid SBA, Basirun WJ, Suhaimy SHM and Mat ANC. A sol-gel derived, copper-doped, titanium dioxide-reduced graphene oxide nanocomposite electrode for the photoelectrocatalytic reduction of CO<sub>2</sub> to methanol and formic acid. *RSC Advances* **5**: 77803-77813 (2015).
42. Cheng J, Zhang M, Wu G, Wang X, Zhou J and Cen K. Optimizing CO<sub>2</sub> reduction conditions to increase carbon atom conversion using a Pt-RGO||Pt TNT photoelectrochemical cell. *Sol. Energy Mater Sol Cells* **132**: 606-614 (2015).
43. Zhang M, Cheng J, Xuan X, Zhou J and Cen, K. Pt/graphene aerogel deposited in Cu foam as a 3D binder-free cathode for CO<sub>2</sub> reduction into liquid chemicals in a TiO<sub>2</sub> photoanode-driven photoelectrochemical cell. *Chem Eng J* **322**: 22-32 (2017).